Mathematical Models of Mechanical Fields in Media with Inclusions and Holes

Marta Bryla, Andrei V. Krupoderov, Alexey A. Kushunin, Vladimir Mityushev and Michail A. Zhuravkov

Abstract Various problems of mechanics described by two-dimensional harmonic and biharmonic functions are investigated by application of the generalized alternating method of Schwarz (GMS). It is demonstrated that the GMS in zeroth approximation coincides with the principle of superposition. Iterative schemes for the $\mathbb{R}$-linear problem on harmonic functions for multiply connected domains are constructed and compared to the GMS. The method is applied in symbolic form to the case when inclusions have elliptical shape. Two-dimensional problems for biharmonic functions by application of the Kolosov–Muskhelishvili formulae are considered by the principle of superposition to describe gas flows in rigid bodies. Viscoelastic problems in porous media are solved by use of the method of finite elements.

Keywords Alternating method of Schwarz · Functional equations for analytic functions · Superposition principle · Elastic half plane with cavities

1 Introduction to the Generalized Alternating Method of Schwarz (GMS)

Mechanical fields considered in this paper are described by two-dimensional harmonic and biharmonic functions. Many problems of the mechanics and of composites are stated as boundary value problems for domains with holes and inclusions when a condition of the contact between the components is written as a conjugation condition for the limit values of the unknown functions and their derivatives [12, 13]. Such problems have been the subject of research interest in porous media and composites

V. Mityushev (✉) · M. Bryla
Department of Computer Sciences and Computer Methods, Pedagogical University, ul. Podchorazych 2, 30-084 Krakow, Poland
e-mail: mityu@up.krakow.pl

A. V. Krupoderov · A. A. Kushunin · M. A. Zhuravkov
Department of Theoretical and Applied Mechanics, Belarusian State University, 4, Nezavisimosti Av., 220030 Minsk, Belarus
e-mail: Zhuravkov@bsu.by

T. M. Rassias (ed.), *Handbook of Functional Equations,*
Springer Optimization and Its Applications 95, DOI 10.1007/978-1-4939-1246-9_2

(e.g. [1, 2, 3, 5, 14, 15, 16]. In the present chapter, attention is paid to the problem of interactions of inclusions and its investigation by the generalized alternating method of Schwarz (GMS) [19, 22, 26].

The main idea of the method can be presented by the $\mathbb{R}$–linear problem on harmonic functions for multiply connected domains. Let D_k be mutually disjoint simply connected domains in the complex plane $\mathbb{C}$ bounded by smooth curves L_k $(k = 1, 2, \ldots, n)$ and D be the complement of all closures of D_k to the extended complex plane $\widehat{\mathbb{C}} = \mathbb{C} \cup \{\infty\}$. Below, the domains D_k are called by inclusions. Denote by D^+ the union of all inclusions D_k, i.e., the domain D^+ consists of n connected components. Let L_k are orientated in a counterclockwise direction. Let ρ be a constant and $c(t)$ be given Hölder continuous functions on $L = \cup_{k=1}^n L_k$, the boundary of D^+.

The $\mathbb{R}$–linear conjugation problem with constant coefficients is stated as follows [22]. To find a function $\varphi(z)$ analytic in D and in all components of D^+, continuous by differentiable in the closures of the considered domains with the following conjugation condition:

$$\varphi^+(t) = \varphi^-(t) - \rho\overline{\varphi^-(t)} + c(t), \quad t \in L. \tag{1}$$

Here $\varphi^\pm(t)$ denotes the limit values of $\varphi(z)$, as z tends to a point $t \in L$ from D^+ and from D, respectively. Moreover, $\varphi(z)$ vanishes at infinity. If $|\rho| < 1$, the problem has a unique solution. This follows from a more general result obtained by Bojarski [6].

In order to describe the GMS we first recall the Sochocki–Plemelj formulae. The curve $L := \cup_{k=1}^n \partial D_k$ divides the complex plane onto domains D^+ and D. Here, each curve ∂D_k is orientated in the clockwise sense. Let $\mu(t)$ be a Hölder continuous function on L. Introduce the function

$$\Phi(z) = \frac{1}{2\pi i}\int_L \frac{\mu(t)}{t-z}dt \tag{2}$$

It is continuous on the complex plane except L where its limit boundary values $\Phi^+(t) = \lim_{z\to t\in D^+}\Phi(z)$ and $\Phi^-(t) = \lim_{z\to t\in D}\Phi(z)$ satisfy the jump condition [11]

$$\Phi^+(t) - \Phi^-(t) = \mu(t), \quad t \in L. \tag{3}$$

The condition (1) can by written in the form (3) with $\Phi^+(t) = \varphi_k(t) - f^+(t)$, $\Phi^-(t) = \varphi(t) - f^-(t)$, $\mu(t) = \rho\overline{\varphi_k(t)}$, where the Cauchy integral

$$f(z) = \frac{1}{2\pi i}\int_L \frac{c(t)}{t-z}\,dt \tag{4}$$

determines the function $f(z)$ analytic outside of L. Then (1) yields

$$\varphi_k(z) = \rho\sum_{m=1}^n \frac{1}{2\pi i}\int_{\partial D_m} \frac{\overline{\varphi_m(t)}}{t-z}dt + f(z).\ z \in D_k, \quad k = 1, 2, \ldots, n. \tag{5}$$

The function $\varphi(z)$ is calculated by $\varphi_m(z)$ as follows:

$$\varphi(z) = \rho \sum_{m=1}^{n} \frac{1}{2\pi i} \int_{\partial D_m} \frac{\overline{\varphi_m(t)}}{t-z} dt + f(z), \quad z \in D. \tag{6}$$

One can consider (5) as a system of integral equations on $\varphi_k(z)$ analytic in D_k and continuously differentiable in its closure. It is worth noting that the equations (5) are not the classic integral equations of the potential theory. They correspond to integral equations which are be deduced from the GMS. In order to analyse (5) we rewrite them in the form

$$\varphi_k(z) - \frac{\rho}{2\pi i} \int_{\partial D_k} \frac{\overline{\varphi_k(t)}}{t-z} dt = \rho \sum_{m \neq k} \frac{1}{2\pi i} \int_{\partial D_m} \frac{\overline{\varphi_m(t)}}{t-z} dt + f(z), z \in D_k, \ k = 1, 2, \ldots, n. \tag{7}$$

The equations (5) can be solved by the following two iterative schemes. First, the direct iterations can be applied to (5)

$$\varphi_k^{(0)}(w) = f(z),$$

$$\varphi_k^{(p+1)}(z) = \rho \sum_{m=1}^{n} \frac{1}{2\pi i} \int_{\partial D_m} \frac{\overline{\varphi_m^{(p)}(t)}}{t-z} dt + f(z), \ z \in D_k, \ k = 1, 2, \ldots, n, \ p = 0, 1, 2, \ldots, \tag{8}$$

where $\varphi_k^{(p)}(w)$ denotes the pth approximation of $\varphi_k(w)$. As it is proved in [21], the iterations (8) uniformly converge for all $|\rho| \leq 1$.

The second iterative scheme is constructed on the basis of the equations (7). The zeroth approximation can be written in the form of the separate equations for each $k = 1, 2, \ldots, n$

$$\varphi_k^{(0)}(z) - \frac{\rho}{2\pi i} \int_{\partial D_k} \frac{\overline{\varphi_k^{(0)}(t)}}{t-z} dt = f(z), \ z \in D_k. \tag{9}$$

According to Bojarski [6], Eq. (9) has a unique solution. The pth approximation has also the form of the equation on $\varphi_k^{(p+1)}(z)$ for each $k = 1, 2, \ldots, n$

$$\varphi_k^{(p+1)}(z) - \frac{\rho}{2\pi i} \int_{\partial D_k} \frac{\overline{\varphi_k^{(p+1)}(t)}}{t-z} dt = \rho \sum_{m \neq k} \frac{1}{2\pi i} \int_{\partial D_m} \frac{\overline{\varphi_m^{(p)}(t)}}{t-z} dt + f(z), z \in D_k. \tag{10}$$

Contrary to the first algorithm (8), convergence results for the second algorithm (9)–(10) are unknown.

The integrals from (10) for $m \neq k$ and $z \in D_k$ can be estimated as follows:

$$\left| \int_{\partial D_m} \frac{\overline{\varphi_m^{(p)}(t)}}{t-z} dt \right| \leq max_{t \in \partial D_m} |\varphi_m^{(p)}(t)| \frac{diam(D_k)}{d_{km}},$$

where $d_{km} = \inf_{t \in \partial D_m \; z \in D_k} |t - z|$, $diam(D_k) = \sup_{z_{1,2} \in D_k} |z_1 - z_2|$.

The values d_{km} and $diam(D_k)$ characterize the distance between D_k and D_m, and the linear size of D_k. If the sum of the ratios

$$\sum_{k=1}^{n} \sum_{m \neq k} \frac{diam(D_k)}{d_{km}} \tag{11}$$

is sufficiently small, the zeroth approximation $\varphi_k^0(z)$ can be accepted as an approximate solution of (5). Then, the approximation for $\varphi(z)$ from (6) becomes

$$\varphi^{(0)}(z) = \rho \sum_{m=1}^{n} \frac{1}{2\pi i} \int_{\partial D_m} \frac{\overline{\varphi_m^{(0)}(t)}}{t-z} dt + f(z), z \in D. \tag{12}$$

Formula (12) expresses the *superposition principle* used in physics when the field in D is approximated by a sum of the separate fields induced by the inclusions D_m. Therefore, the GMS applied within the zeroth approximation yields the superposition principle. In Sect. 3, this principle is applied to complicated mechanical fields.

2 R–Linear Problem with Elliptical Inclusions

The present section is devoted to application of the GMS to the $\mathbb{R}$–linear problem with many inclusions of elliptic shapes. We follow Sect. 1 and the paper [20] where this problem was considered in the case when all the ellipses have the same shape. In this section, we consider the general case when each ellipse can have arbitrary semi-axes and arbitrary size.

2.1 Statement of the Problem and Reduction to Integral Equations

Suppose that the elliptical inclusions $D_m (m = 1, 2, \ldots, n)$ do not overlap. For convenience, put the semiaxes equal to $r_m(1 + \alpha_m)$ and $r_m(1 - \alpha_m)$, respectively. The parameter r_m is positive and characterizes the size of inclusion, and α_m is the shape of the mth ellipse ($0 < \alpha_m < 1$). The case $\alpha_m = \alpha$ ($m = 1, 2, \ldots, n$) was considered in [20]. Let an inclusion D_m be centred at (x_m, y_m) and the angle between the major semiaxis of the ellipse and the x-axis be equal to θ_m. In accordance with Mityushev [20], introduce the local coordinates (X, Y) for a fixed inclusion D_m as follows:

$$X = \frac{1}{r_m} [(x - x_m) \cos\theta_m + (y - y_m) \sin\theta_m], \tag{13}$$

$$Y = \frac{1}{r_m}[(x - x_m)\sin\theta_m + (y - y_m)\cos\theta_m]. \tag{14}$$

The local equation of the ellipse ∂D_m has the form

$$\frac{X^2}{(1+\alpha_m)^2} + \frac{Y^2}{(1-\alpha_m)^2} = 1. \tag{15}$$

The foci of the ellipse ∂D_m in the local coordinates are located at $(\pm 2\sqrt{\alpha_m}, 0)$.

Let $Z = X + iY$ be the local complex coordinate, $z = x + iy$ and $w = \xi + i\zeta$ be global complex coordinates, where i denotes the imaginary unit. The Joukowsky conformal mapping

$$Z = w + \frac{\alpha_m}{w} \tag{16}$$

transforms the annulus $\sqrt{\alpha_m} < |w| < 1$ onto $D_m - \Gamma_m$, where Γ_m denotes the slit $(-2\sqrt{\alpha_m}, 2\sqrt{\alpha_m})$ along the X-axis. The inverse mapping to (16) has the form

$$w = \frac{1}{2}\left(Z + \sqrt{Z^2 - 4\alpha_m}\right) \tag{17}$$

where the branch of the square root is chosen in such a way that

$$\lim_{X \to \pm i0} \sqrt{Z^2 - 4\alpha_m} = \pm i\sqrt{4\alpha_m - X^2} \tag{18}$$

for $-2\sqrt{\alpha_m} < X < 2\sqrt{\alpha_m}$. Formulae (16)–(17) in the global coordinates become

$$z = s_m(w + \frac{\alpha_m}{w} + a_m) \tag{19}$$

$$w = \frac{1}{2}\left[\frac{z - a_m}{s_m} + \sqrt{\left(\frac{z - a_m}{s_m}\right)^2 - 4\alpha_m}\right], \tag{20}$$

where $s_m = r_m e^{i\theta_m}$.

Let D denote the complement of the closures of all domains D_m to the extended complex plane. We study the conductivity of the two-dimensional composite, when the domains D and D_m are occupied by materials of unit and λ conductivity, respectively, where $0 < \lambda < \infty$. Then, the potentials $u(z)$ and $u_m(z)$ are harmonic in D and D_m $(m = 1, 2, \ldots n)$ and satisfies the conjugation (transmission) conditions

$$u = u_m,\ \frac{\partial u}{\partial n} = \lambda \frac{\partial u_m}{\partial n},\ \text{on } \partial D_m,\ m = 1, 2, \ldots, n, \tag{21}$$

where $\partial/\partial n$ denotes the outward normal derivative to the ellipses. For simplicity, it is assumed that the potential $u(z)$ has singularities only in the domain D described by a function $Re f(z)$, where $f(z)$ is analytic in all inclusions D_k, Re stands for the real part of a complex number.

Following Mityushev and Rogosin [22], introduce complex potentials $\varphi(z)$ and $\varphi_m(z)$ analytic in D and D_m, respectively, in such a way that $u(z)$ and $u_m(z)$ are related to the complex potentials by

$$u(z) = Re[\varphi(z) + f(z)],\, u_m(z) = \frac{2}{1+\lambda} Re\varphi_m(z). \tag{22}$$

Then the conditions (21) can by reduced to the $\mathbb{R}$-linear problem (1), where $c(t) = f(z)$ and ρ denotes the contrast parameter

$$\rho = \frac{\lambda - 1}{\lambda + 1}. \tag{23}$$

2.2 Solution to Integral Equations

It follows from Sect. 1 that the $\mathbb{R}$-linear problem (1) is reduced to the integral equations (5). We now reduce these equations for elliptic inclusions to a system of functional equations (without integral terms).

Let k be fixed in (5). The doubly connected domain $D_k - \Gamma_k$ is mapped onto the annulus $\sqrt{\alpha_k} < |w| < 1$ by the conformal mapping (20); D_k is transformed onto the unit circle $|w| = 1$, Γ_k onto the circle $|w| = \sqrt{\alpha_k}$. Introduce the functions

$$\Phi_k(w) = \varphi_k(z) = \varphi_k\left[s_k\left(w + \frac{\alpha_k}{w}\right) + a_k\right] \tag{24}$$

analytic in $\sqrt{\alpha_k} < |w| < 1$ and continuous in $\sqrt{\alpha_k} \le |w| \le 1$. Substitute (24) in (5) and change the variables in the integrals as follows:

$$t = s_k\left(\tau + \frac{\alpha_k}{\tau}\right) + a_k. \tag{25}$$

Then (5) becomes

$$\Phi_k(w) = \rho \sum_{m=1}^{n} \frac{1}{2\pi i} \int_{|\tau|=1} \frac{\overline{\Phi_m(\tau)}(1 - \frac{\alpha_m}{\tau^2})d\tau}{\tau + \frac{\alpha_m}{\tau} - \frac{s_k}{s_m}(w + \frac{\alpha_k}{w}) + \frac{a_m - a_k}{s_m}} + F(w), \tag{26}$$

$$\sqrt{\alpha_k} < |w| < 1, \quad k = 1, 2, \ldots, n,$$

where $F(w) = f(z)$. Moreover, it follows from the continuity of $\varphi_k(z)$ when z passes the slit Γ_k that

$$\Phi_k(\tau) = \Phi_k\left(\frac{\alpha_k}{\tau}\right), \quad |\tau| = \sqrt{\alpha_k}. \tag{27}$$

Equation (27) implies that $\Phi_k(w)$ is represented in the form

$$\Phi_k(w) = \phi_k(w) + \phi_k\left(\frac{\alpha_k}{w}\right), \quad \alpha_k \le |w| \le 1, \tag{28}$$

where $\phi_k(w)$ is analytic in the unit disk $|w| < 1$. Equation (28) follows from the representation of $\Phi_k(w)$ in the form of the Laurent series in the annulus $\alpha_k \le |w| \le 1$ and form (27). The same arguments yield the representation of $F(w)$ in the form $F(w) = g_k(w) + g_k(\frac{\alpha_k}{w})$, where $g_k(w)$ is analytic in the unit disk. Substitution of (28) into (26) yields

$$\phi_k(w) + \phi_k\left(\frac{\alpha_k}{w}\right) = \rho \sum_{m=1}^{n} \Big[P_{km}(w) + Q_{km}(w) \Big] + g_k(w) + g_k\left(\frac{\alpha_k}{w}\right), \quad (29)$$

$$\alpha_k < |w| < 1, \quad k = 1, 2, \ldots, n,$$

where

$$P_{km}(w) = \frac{1}{2\pi i} \int_{|\tau|=1} \frac{\overline{\phi_m(\frac{1}{\overline{\tau}})}(1 - \frac{\alpha_m}{\tau^2}) d\tau}{\tau + \frac{\alpha_m}{\tau} - \frac{s_k}{s_m}(w + \frac{\alpha_k}{w}) + \frac{a_m - a_k}{s_m}}, \quad (30)$$

$$Q_{km}(w) = \frac{1}{2\pi i} \int_{|\tau|=1} \frac{\overline{\phi_m(\alpha_m \overline{\tau})}(1 - \frac{\alpha_m}{\tau^2}) d\tau}{\tau + \frac{\alpha_m}{\tau} - \frac{s_k}{s_m}(w + \frac{\alpha_k}{w}) + \frac{a_m - a_k}{s_m}}. \quad (31)$$

Here, the relation $\overline{\tau} = \frac{1}{\tau}$ on the unit circle is used.

The integrals (30)–(31) are analytically calculated by residues in [20]. Following [20] consider the quadratic equation with respect to τ

$$\tau^2 - s_m^{-1} \left[s_k \left(w + \frac{\alpha_k}{w} \right) + a_k - a_m \right] \tau + \alpha_m = 0. \quad (32)$$

The cases of equal and non equal k and m have to be separately investigated.
a) Let $k = m$. Then Eq. (32) becomes

$$\tau^2 - \left(w + \frac{\alpha_k}{w} \right) \tau + \alpha_k = 0. \quad (33)$$

Its two solutions have the form

$$\tau_1 = w, \; \tau_2 = \frac{\alpha_k}{w}. \quad (34)$$

b) Let $k \neq m$. In order to avoid a confusion with (34), the roots of (32) in this case are denoted by w_1 and w_2

$$w_1 = \frac{1}{2} \left\{ s_m^{-1} \left[\left(w + \frac{\alpha_k}{w} \right) + a_k - a_m \right] - \sqrt{\left[\frac{s_k(w + \frac{\alpha_k}{w}) + a_k - a_m}{s_m} \right]^2 - 4\alpha_m} \right\} \quad (35)$$

$$w_2 = \frac{1}{2} \left\{ s_m^{-1} \left[s_k \left(w + \frac{\alpha_k}{w} \right) + a_k - a_m \right] + \sqrt{\left[\frac{s_k(w + \frac{\alpha_k}{w}) + a_k - a_m}{s_m} \right]^2 - 4\alpha_m} \right\}$$

The branch of the square root is chosen in accordance with (18). It was proved in [20] that $|w_1| < 1$ and $|w_2| > 1$.

The integrals (30)–(31) were calculated in [20]. From $m \neq k$ it can be written in the form

$$P_{km}(w) = \overline{\phi_m(0)} - \overline{\phi_m\left(\frac{\overline{w}_1}{\alpha_m}\right)}, \quad (m \neq k), \quad P_{kk}(w) = \overline{\phi_k(0)},$$

$$Q_{km}(w) = \overline{\phi_m(0)} - \overline{\phi_m(\alpha_m w_1)} \quad (m \neq k), Q_{kk}(w) = \overline{-\phi_k(0)} + \overline{\phi_k(\alpha_k \overline{w})} + \overline{\phi_k\left(\frac{\alpha_k^2}{\overline{w}}\right)},$$

where w_1 and w_2 are given by (35).

2.3 Functional Equations

Substituting (34)–(35) into (29) we transform the integral equations (29) to the following functional equations:

$$\phi_k(w) + \phi_k\left(\frac{\alpha_k}{w}\right) = \rho\Bigg\{\overline{\phi_k(\alpha_k \overline{w})} + \overline{\phi_k\left(\frac{\alpha_k^2}{\overline{w}}\right)} - \tag{36}$$

$$- \sum_{m \neq k}\left[-2\overline{\phi_m(0)} + \overline{\phi_m(\alpha_m \overline{\beta_{km}(w)})} + \overline{\phi_m\left(\frac{\overline{\beta_{km}(w)}}{\alpha_m}\right)}\right] + g_k(w) + g_k\left(\frac{\alpha_m(w)}{w}\right)\Bigg\},$$

$$\sqrt{\alpha_k} < |w| < 1, \quad k = 1, 2, \ldots, n.$$

Here, for convenience the root w_1 is written as the function of w

$$\beta_{km}(w) = \frac{1}{2}\left\{s_m^{-1}\left[s_k\left(w + \frac{\alpha_k}{w}\right) + a_k - a_m\right] - \sqrt{h_{km}(w)}\right\}, \tag{37}$$

where

$$h_{km}(w) = \left[\frac{s_k(w + \frac{\alpha_k}{w}) + a_k - a_m}{s_m}\right]^2 - 4\alpha_m. \tag{38}$$

The right hand part of (36) consists of the functions $\phi_k(w)$ and $\phi_k\left(\frac{\alpha_m}{w}\right)$ analytic in $|w| < 1$ and $|w| > \sqrt{\alpha_m}$, respectively. Denote by P^+ the project operator which transforms a function analytic in $\sqrt{\alpha_m} < |w| < 1$ to its part analytic in the unit disk. This operator can by considered as taking the regular part of the Laurent series or as the integral operator $\frac{1}{2\pi i}\int_{|w|=1} \frac{\bullet\, dw}{w-\zeta}$ with $|\zeta| < 1$. Application of P^+ to (36) yields

$$\phi_k(w) + \phi_k(0) = \rho\Big\{\overline{\phi_k(\alpha_m \overline{w})} + \overline{\phi_k(0)} - \tag{39}$$
$$\sum_{m\neq k}\left[-2\overline{\phi_m(0)} + P^+\overline{\phi_m(\alpha_m \overline{\beta_{km}(w)})} + P^+\overline{\phi_m\left(\frac{\overline{\beta_{km}(w)}}{\alpha_m}\right)}\right] + g_k(w) + g_k(0)\Big\},$$

$$|w| \le 1,\ k = 1, 2, \ldots, n.$$

Here, the following relation is used:

$$P^+\overline{\phi_k\left(\frac{\alpha_k^2}{\overline{w}}\right)} = \overline{\phi_k(0)}.$$

One can consider (39) as a system of functional equations on the functions $\phi_k(w)$ analytic in the unit disk and continuous in its closure. The solution of (39) can be found by the method of successive approximations corresponding to the algorithm (8). The equations (39) can by considered as iterative functional equations with shift into domain [20, 22], since $|\beta_{km}(w)| < 1$. It is worth noting that the equations (39) do not contain integral terms and can be solved by use of the symbolic computations, hence, the obtained results can be obtained in the form of approximate analytical formulae.

3 Some Model Problems of Gas Flows in Rigid Bodies

3.1 Stress–Strain State of the Elastic Half Plane with Holes Filled by Gas

One of the mathematical model approaches to creation describe the stress–strain state of an elastic half plane with cavities that can contain gas, is discussed in this section. We consider an elastic isotropic half plane with two holes which are far away from the half-plane boundary and each other. This assumption allows us to apply the GMS in the zeroth approximation (the method of superposition discussed in Sect. 1). All the problems are considered in the plain strain condition. One of the holes is a circle with radius R and centre at the origin. The second hole is an ellipse with semiaxes a and b. The centre of the ellipse is placed at the point $O_1(x_{01}, y_{01})$. The x-axis forms the angle ϵ with O_1O (see Fig. 1). Let the real axis and the boundary of holes be denoted by L_0, L_1, L_2, respectively, and the distance from the centre of the circle to L_0 be H. Let the homogeneous pressure p_0 be given on the boundary L_1 and boundaries L_0 and L_2 be free.

The Kolosov–Muskhelishvili method will be used to solve this problem. Let S^* be a domain bounded by contours L_0, L_1, L_2 and S a domain bounded by L_1 and L_2. The problem is described by the following equilibrium equations:

$$\frac{\partial\sigma_x^{(1)}}{\partial x} + \frac{\partial\tau_{xy}^{(1)}}{\partial y} = 0,$$

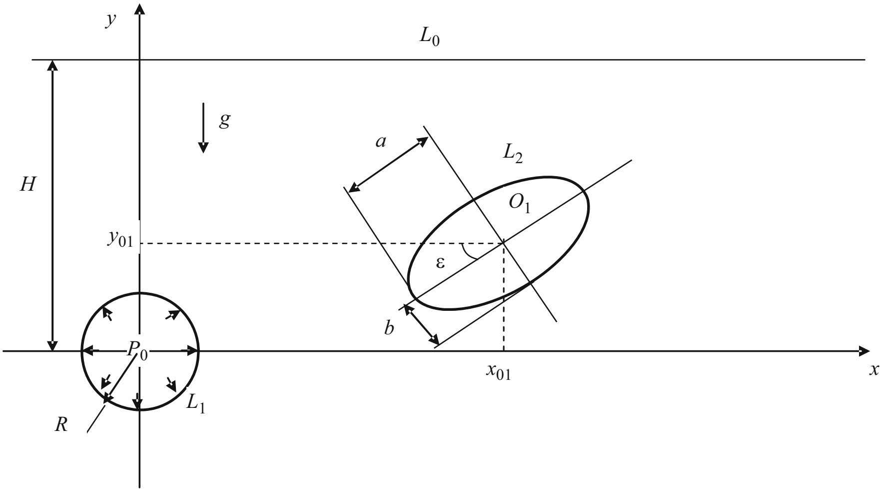

Fig. 1 Scheme of model problem

$$\frac{\partial \tau_{xy}^{(1)}}{\partial x} + \frac{\partial \sigma_y^{(1)}}{\partial y} - \rho g = 0,$$
$$\Delta(\sigma_x^{(1)} + \sigma_y^{(1)}) = 0 \tag{40}$$

and the boundary conditions

$$\sigma_x^{(1)} \cos(n, x) + \tau_{xy}^{(1)} \cos(n, y) = 0,\ \tau_{xy}^{(1)} \cos(n, x) + \sigma_y^{(1)} \cos(n, y) = 0$$
$$\text{on } L_j\ (j = 0, 2), \tag{41}$$

$$\sigma_x^{(1)} \cos(n, x) + \tau_{xy}^{(1)} \cos(n, y) = -P_0 \cos(n, x),$$
$$\tau_{xy}^{(1)} \cos(n, x) + \sigma_y^{(1)} \cos(n, y) = -P_0 \cos(n, y) \text{ on } L_1, \tag{42}$$

where σ_{ij} denote the stress components, ρ the media density, g the gravity acceleration, and n the outward normal to the boundaries L_j.

Using the superposition principle we can represent the stress components as follows:

$$\sigma_x^{(1)} = \sigma_x^{(0)} + \sigma_x, \tau_{xy}^{(1)} = \tau_{xy}^{0} + \tau_{xy}, \sigma_y^{(1)} = \sigma_y^{(0)} + \sigma_y, \tag{43}$$

The sizes of holes are small in comparison with plane sizes. Therefore stresses σ_{ij} are negligible at large distance from holes, hence, σ_{ij} vanish at infinity. It is evident that the additional stresses satisfy homogeneous equilibrium equations. If the boundaries L_1 and L_2 are far away from the boundary L_0, we can consider an infinite plane with holes. The formulae for initial stresses are well known

$$\sigma_x^{(0)} = \rho g(y - H), \tau_{xy}^{(0)} = 0, \sigma_y^{(0)} = \lambda \rho g(y - H),$$

where λ is the ratio of horizontal to vertical stress.

The boundary conditions for the additional stresses have the form

$$\sigma_y = \tau_{xy} = 0 \text{ on } L_0; \tag{44}$$

$$\sigma_x \cos(n, x) + \tau_{xy} \cos(n, y) = f_i \cos(n, x),$$

$$\tau_{xy} \cos(n, x) + \sigma_y \cos(n, y) = g_i \cos(n, y) \text{ on } L_j,\ j = 1, 2,$$

where

$$f_1 = p\rho g H - P_0,\ g_1 = \rho g H - P_0,\ f_2 = p\rho g(H - y_{01}),\ g_2 = \rho g(H - y_{01}).$$

Following the Kolosov–Mushelishvili method we use the complex potentials $\Phi(z)$ and $\Psi(z)$

$$\sigma_x + \sigma_y = 2(\Phi(z) - \overline{\Phi(z)}), \sigma_y - \sigma_x + 2\tau_{xy} = 2(\overline{z}\Phi'(z) - \Psi(z)).$$

Using the superposition principle and the well-known solutions for infinite plane with elliptic and circular holes [23, 30] (with $p = 1$), we obtain

$$\sigma_x = Re[-\Psi_1(x) + 2\Phi_2(z_1) - K(z_1)],$$

$$\tau_{xy} = Im[\Psi_1(z) + K(z_1)],$$

$$\sigma_y = Re[\Psi_1(z) + 2\Phi_2(z_1) + K(z_1)],$$

where

$\Psi_1(z) = \frac{P_1 R^2}{z^2}$, $z = x + iy$, $\Phi_2(z_1) = \frac{\varphi_2'(\varsigma)}{\omega'(\varsigma)}$, $z_1 = e^{-is}(z - z_{01})$, $K(z_1) = e^{-2is}(\overline{z_1}\Phi_2'(z_1) + \Psi_2(z_1))$, $P_1 = P_0 - \rho g h$, $z_{01} = x_{01} + iy_{01}$, $\varphi'(\varsigma) = \frac{\omega'(\varsigma)\varphi_2''(\varsigma) - \varphi_2'(\varsigma)\omega''(\varsigma)}{(\omega'(\varsigma))^2}$, $\varphi_2(\varsigma) = \frac{P_2 E s}{\varsigma}$, $E = \frac{a+b}{2}$, $s = \frac{a-b}{a+b}$, $\omega(\varsigma) = E(\varsigma + s/\varsigma)$, $\varsigma = \frac{z_1 + \sqrt{z_1^2 - 4E^2\ s}}{2E}$, $\Psi_2(z_1) = \frac{\psi_2'(\varsigma)}{\omega'(\varsigma)}$, $\psi_2 = \frac{P_2 E}{\varsigma} + \frac{P_2 E s}{\varsigma} \frac{1 + s\varsigma^2}{\varsigma^2 - s}$, $P_2 = \rho g(H - y_{01})$, $\Phi_2'(z_1) = \frac{\varphi'(\varsigma)}{\omega'(\varsigma)}$.

The main stresses become

$$\sigma_1 = \frac{\sigma_x^{(1)} + \sigma_y^{(1)}}{2} + \frac{\sigma_x^{(1)} - \sigma_y^{(1)}}{2} \cos(2\theta) + \tau_{xy}^{(1)} \sin(2\theta),$$

$$\sigma_2 = \frac{\sigma_x^{(1)} + \sigma_y^{(1)}}{2} - \frac{\sigma_x^{(1)} - \sigma_y^{(1)}}{2} \cos(2\theta) - \tau_{xy}^{(1)} \sin(2\theta),$$

$$\sigma_3 = \nu(\sigma_x^{(1)} + \sigma_y^{(1)}), \tag{45}$$

where $\theta = \frac{1}{2} \arctan \frac{2\tau_{xy}^{(1)}}{\sigma_x^{(1)} - \sigma_y^{(1)}}$ and ν denotes Poisson's ratio. Solutions to these problems by other methods are described in [7, 18, 28, 29].

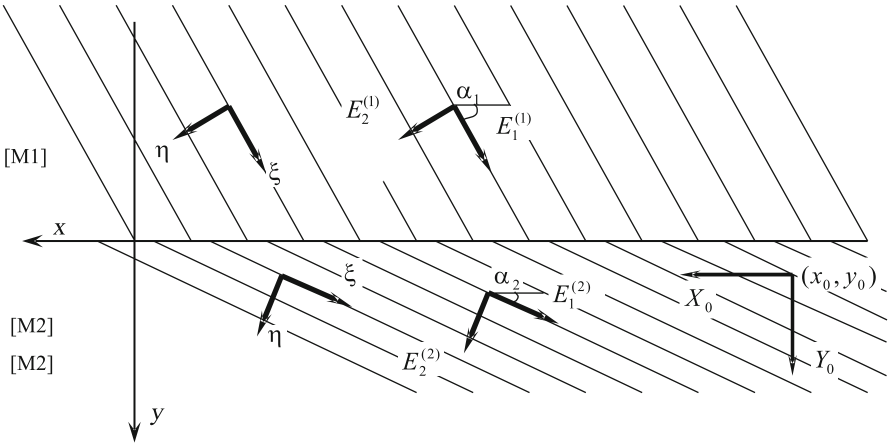

Fig. 2 Scheme of model problem for two orthotropic half planes

3.2 Stress–Strain State of the Rock Massif and Applications to Gas Dynamic Phenomena

We consider an orthotropic elastic body which consists of two half planes D_j $(j = 1, 2)$ with different elastic constants. The line $y = 0$ be the boundary between the half planes and let the y-axis be directed downward. Each half plane is orthotropic in the local coordinate system (ξ, η) as displayed in Fig. 2.

Hooke's law in the local coordinate system becomes

$$\begin{aligned} \frac{\partial U^{(j)}}{\partial \xi} &= \beta_{11}^{(j)} \sigma_\xi^{(j)} + \beta_{12}^{(j)} \sigma_\eta^{(j)}, \\ \frac{\partial V^{(j)}}{\partial \eta} &= \beta_{12}^{(j)} \sigma_\xi^{(j)} + \beta_{22}^{(j)} \sigma_\eta^{(j)}, \\ \frac{\partial U^{(j)}}{\partial \eta} + \frac{\partial V^{(j)}}{\partial \xi} &= \beta_{66}^{(j)} \tau_{\xi\eta}^{(j)}. \end{aligned} \tag{46}$$

where

$$\beta_{11}^{(j)} = \frac{1 - \nu_{31}^{(j)} \nu_{13}^{(j)}}{E_1^{(j)}}, \beta_{12}^{(j)} = -\frac{\nu_{21}^{(j)} + \nu_{31}^{(j)} \nu_{23}^{(j)}}{E_2^{(j)}}, \beta_{22}^{(j)} = \frac{1 - \nu_{23}^{(j)} \nu_{32}^{(j)}}{E_2^{(j)}}, \beta_{66}^{(j)} = \frac{1}{G_{12}^{(j)}}.$$

E_1^j and E_2^j are Young's modules in the principal directions ξ and η, respectively. Here, G_{12}^j denotes the shear modulus in the plain (ξ, η), ν_{kl}^j Poisson's coefficients. The angle between the local and global coordinate systems is denoted by α_j.

Hooke's law in the main coordinate system can be written in the form

$$\frac{\partial U^{(j)}}{\partial x} = c_{11}^{(j)}\sigma_x^{(j)} + c_{12}^{(j)}\sigma_y^{(j)} + c_{16}^{(j)}\tau_{xy}^{(j)},$$
$$\frac{\partial V^{(j)}}{\partial y} = c_{12}^{(j)}\sigma_x^{(j)} + c_{22}^{(j)}\sigma_y^{(j)} + c_{26}^{(j)}\tau_{xy}^{(j)},$$
$$\frac{\partial U^{(j)}}{\partial y} + \frac{\partial V^{(j)}}{\partial x} = c_{16}^{(j)}\sigma_x^{(j)} + c_{26}^{(j)}\sigma_y^{(j)} + c_{66}^{(j)}\tau_{xy}^{(j)}. \quad (47)$$

The coefficients c_{mn} linearly depend on the coefficients β_{kl} as follows:

$$c_{11}^{(j)} = \beta_{11}^{(j)}\cos^4(\alpha_j) + B^{(j)}\sin^2(\alpha_j)\cos^2(\alpha_j) + \beta_{22}^{(j)}\sin^4(\alpha_j),$$
$$c_{22}^{(j)} = \beta_{11}^{(j)}\sin^4(\alpha_j) + B^{(j)}\sin^2(\alpha_j)\cos^2(\alpha_j) + \beta_{22}^{(j)}\cos^4(\alpha_j),$$
$$c_{12}^{(j)} = \beta_{12}^{(j)} + (\beta_{11}^{(j)} + \beta_{22}^{(j)} - B^{(j)})\sin^2(\alpha_j)\cos^2(\alpha_j),$$
$$c_{66}^{(j)} = \beta_{66}^{(j)} + 4(\beta_{11}^{(j)} + \beta_{22}^{(j)} - B^{(j)})\sin^2(\alpha_j)\cos^2(\alpha_j),$$
$$c_{16}^{(j)} = (2\beta_{22}^{(j)}\sin^2(\alpha_j) - 2\beta_{11}^{(j)}\cos^2(\alpha_j) + B^{(j)}\cos(2\alpha_j))\sin(\alpha_j)\cos(\alpha_j),$$
$$c_{26}^{(j)} = (2\beta_{22}^{(j)}\cos^2(\alpha_j) - 2\beta_{11}^{(j)}\sin^2(\alpha_j) - B^{(j)}\cos(2\alpha_j))\sin(\alpha_j)\cos(\alpha_j),$$

where $B^{(j)} = 2\beta_{12}^{(j)} + \beta_{66}^{(j)}$.

We will solve the problem when the body forces are absent. Then, the equilibrium equations become

$$\frac{\partial \sigma_x^{(j)}}{\partial x} + \frac{\partial \tau_{xy}^{(j)}}{\partial y} = 0,$$
$$\frac{\partial \tau_{xy}^{(j)}}{\partial x} + \frac{\partial \sigma_y^{(j)}}{\partial y} = 0. \quad (48)$$

The stress tensor components can be written in the form

$$\sigma_x^{(j)} = \frac{\partial^2 W^{(j)}}{\partial y^2},\ \sigma_y^{(j)} = \frac{\partial^2 W^{(j)}}{\partial x^2},\ \tau_{xy}^{(j)} = -\frac{\partial^2 W^{(j)}}{\partial y \partial x}, \quad (49)$$

where $W^{(j)}$ denotes the Airy function. Then, the equilibrium equations are satisfied and the compatibility equation becomes

$$c_{22}^{(j)}\frac{\partial^4 W^{(j)}}{\partial x^4} - 2c_{26}^{(j)}\frac{\partial^4 W^{(j)}}{\partial x^3 \partial y} + (2c_{12}^{(j)} + c_{66}^{(j)})\frac{\partial^4 W^{(j)}}{\partial x^2 \partial y^2} - 2c_{16}^{(j)}\frac{\partial^4 W^{(j)}}{\partial x \partial y^3} + c_{11}^{(j)}\frac{\partial^4 W^{(j)}}{\partial y^4} = 0. \quad (50)$$

We use the following representation for the function W [9]

$$W^{(j)} = 2Re[F_1^{(j)}(z_1^{(j)}) + F_2^{(j)}(z_2^{(j)})], \quad (51)$$

where $F_i^{(j)}$ are analytical functions of the complex argument $z_k^j = x + \mu_k^j y (k = 1, 2)$. The constants μ_k^j will be defined below.

We introduce the functions

$$\frac{dF_1^{(j)}(z)}{dz} = \varphi_1^{(j)}(z), \frac{dF_2^{(j)}(z)}{dz} = \varphi_2^{(j)}(z),$$
$$\frac{d\varphi_1^{(j)}(z)}{dz} = \Phi_1^{(j)}(z), \frac{d\varphi_2^{(j)}(z)}{dz} = \Phi_2^{(j)}(z).$$

Then, the stress components are calculated by the following formulae:

$$\begin{aligned}\sigma_x^{(j)} &= 2Re[(\mu_1^{(j)})^2\Phi_1^{(j)}(z_1^{(j)}) + (\mu_2^{(j)})^2\Phi_2^{(j)}(z_2^{(j)})],\\ \sigma_y^{(j)} &= 2Re[\Phi_1^{(j)}(z_1^{(j)}) + \Phi_2^{(j)}(z_2^{(j)})],\\ \tau_{xy}^{(j)} &= -2Re[\mu_1^{(j)}\Phi_1^{(j)}(z_1^{(j)}) + \mu_2^{(j)}\Phi_2^{(j)}(z_2^{(j)})].\end{aligned} \quad (52)$$

The displacements components become

$$\begin{aligned}U^{(j)} &= 2Re[p_1^{(j)}\varphi_1^{(j)}(z_1^{(j)}) + p_2^{(j)}\varphi_2^{(j)}(z_2^{(j)})],\\ V^{(j)} &= 2Re[q_1^{(j)}\varphi_1^{(j)}(z_1^{(j)}) + q_2^{(j)}\varphi_2^{(j)}(z_2^{(j)})],\end{aligned} \quad (53)$$

where $p_k^{(j)} = c_{11}^{(j)}(\mu_k^{(j)})^2 + c_{12}^{(j)} - c_{16}^{(j)}\mu_k^{(j)}$, $\mu_k^{(j)}q_k^{(j)} = c_{11}^{(j)}(\mu_k^{(j)})^2 + c_{22}^{(j)} - c_{26}^{(j)}\mu_k^{(j)}$.

The compatibility equation (50) with (52) and (53) yields

$$c_{11}^{(j)}\mu^4 - 2c_{16}^{(j)}\mu^3 + (2c_{12}^{(j)} + c_{66}^{(j)})\mu^2 - 2c_{26}^{(j)}\mu + c_{22}^{(j)} = 0. \quad (54)$$

As shown in [17] this equation has two pairs of complex conjugate roots.

Let a concentrated force be applied at a point $M_0(X_0, Y_0)$ of the domain D_j. Then, the complex potentials in a neighbourhood of this point become

$$\begin{aligned}\varphi_1^{(j)}(z_1^{(j)}) &= a_0^{(j)}\ln(z_1^{(j)} - \tau_1^{(j)}) + \varphi_*^{(j)}(z_1^{(j)}), z_1^{(j)} \to \tau_1^{(j)},\\ \varphi_2^{(j)}(z_2^{(j)}) &= b_0^{(j)}\ln(z_2^{(j)} - \tau_2^{(j)}) + \psi_*^{(j)}(z_2^{(j)}), z_2^{(j)} \to \tau_2^{(j)},\end{aligned} \quad (55)$$

where $\varphi_*^{(j)}(z_1^{(j)})$ and $\psi_*^{(j)}(z_2^{(j)})$ are holomorphic functions in a vicinity of the point M_0.

The coefficients $a_0^{(j)}, b_0^{(j)}$ are calculated by formulae [24]

$$\begin{aligned}a_0^{(j)} &= \frac{i(X_0 + \mu_2^{(j)}Y_0) + m^{(j)} - n^{(j)}\mu_2^{(j)}}{4\pi(\mu_1^{(j)} - \mu_2^{(j)})},\\ b_0^{(j)} &= -\frac{i(X_0 + \mu_1^{(j)}Y_0) + m^{(j)} - n^{(j)}\mu_1^{(j)}}{4\pi(\mu_1^{(j)} - \mu_2^{(j)})},\end{aligned} \quad (56)$$

where $m^{(j)} = \frac{k_0^{(j)}(\delta_1^{(j)}X_0 - \delta_3^{(j)}Y_0)}{(\delta_1^{(j)})^2 + \delta_2^{(j)}\delta_3^{(j)}}$, $n^{(j)} = \frac{k_0^{(j)}(\delta_2^{(j)}X_0 + \delta_1^{(j)}Y_0)}{(\delta_1^{(j)})^2 + \delta_2^{(j)}\delta_3^{(j)}}$, $\delta_1^{(j)} = Im[\mu_1^{(j)}\mu_2^{(j)}]$, $\delta_2^{(j)} = Im[\mu_1^{(j)} + \mu_2^{(j)}]$, $\delta_3^{(j)} = Im[(\mu_1^{(j)} + \mu_2^{(j)})\overline{\mu_1^{(j)}\mu_2^{(j)}}]$, $k_0^{(j)} = Re[\mu_1^{(j)}\mu_2^{(j)}] - \frac{c_{12}^{(j)}}{c_{11}^{(j)}}$.

3.2.1 Fundamental Solution

We determine the stress–strain state of the described body loaded by a concentrated force P applied at the point $M_0(x_0, y_0)$. It is assumed that the condition of the ideal contact on the line $y = 0$ takes place

$$\sigma_y^{(1)} = \sigma_y^{(2)},\ \tau_{xy}^{(1)} = \tau_{xy}^{(2)},\ U^{(1)} = U^{(2)},\ V^{(1)} = V^{(2)} \tag{57}$$

and all the stresses vanish at infinity.

The following stress functions are used:

$$\begin{aligned}
\Phi_1^{(1)}(z_1^{(1)}) &= \frac{s_1}{z_1^{(1)} - \tau_1^{(2)}} + \frac{s_2}{z_1^{(1)} - \tau_2^{(2)}},\\
\Phi_2^{(1)}(z_2^{(1)}) &= \frac{l_1}{z_2^{(2)} - \tau_1^{(2)}} + \frac{l_2}{z_2^{(2)} - \tau_2^{(2)}},\\
\Phi_1^{(2)}(z_1^{(2)}) &= \frac{a_0^{(2)}}{z_1^{(2)} - \tau_1^{(2)}} + \frac{n_1}{z_1^{(2)} - \overline{\tau_1^{(2)}}} + \frac{n_2}{z_1^{(2)} - \overline{\tau_2^{(2)}}},\\
\Phi_2^{(2)}(z_2^{(2)}) &= \frac{b_0^{(2)}}{z_2^{(2)} - \tau_2^{(2)}} + \frac{m_1}{z_2^{(2)} - \overline{\tau_1^{(2)}}} + \frac{m_2}{z_2^{(2)} - \overline{\tau_2^{(2)}}},
\end{aligned} \tag{58}$$

where s_1, s_2, l_1, l_2, n_1, n_2, m_1, and m_2 are arbitrary coefficients. The coefficients s_i, l_i, n_i, and m_i are defined by the equations (57). Consider the case when $\sigma_y^{(1)} = \sigma_y^{(2)}$. For $y = 0$, we have

$$\sigma_y^{(1)} = 2Re\left[\frac{s_1}{x - \tau_1^{(2)}} + \frac{s_2}{x - \tau_2^{(2)}} + \frac{l_1}{x - \tau_1^{(2)}} + \frac{l_2}{x - \tau_2^{(2)}}\right],$$

$$\sigma_y^{(2)} = Re\left[\frac{a_0^{(2)}}{x - \tau_1^{(2)}} + \frac{n_1}{x - \overline{\tau_1^{(2)}}} + \frac{n_2}{x - \overline{\tau_2^{(2)}}} + \frac{b_0^{(2)}}{x - \tau_2^{(2)}} + \frac{m_1}{x - \overline{\tau_1^{(2)}}} + \frac{m_2}{x - \overline{\tau_2^{(2)}}}\right].$$

Comparing the coefficients at $\frac{1}{1-\tau_1^2}$ and $\frac{1}{1-\tau_2^2}$ we obtain, respectively

$$s_1 + l_1 - \overline{n_1} - \overline{m_1} = a_0^{(2)}, \quad s_2 + l_2 - \overline{n_2} - \overline{m_2} = b_0^{(2)}.$$

Thus, the coefficients satisfy the following system of equations:

$$\begin{aligned}
s_1 + l_1 - \overline{n_1} - \overline{m_1} &= a_0^{(2)},\\
\mu_1^{(1)} s_1 + \mu_2^{(1)} l_1 - \overline{\mu_1^{(2)}}\,\overline{n_1} - \overline{\mu_2^{(2)}}\,\overline{m_1} &= \mu_1^{(2)} a_0^{(2)},\\
p_1^{(1)} s_1 + p_2^{(1)} l_1 - \overline{p_1^{(2)}}\,\overline{n_1} - \overline{p_2^{(2)}}\,\overline{m_1} &= p_1^{(2)} a_0^{(2)},\\
q_1^{(1)} s_1 + q_2^{(1)} l_1 - \overline{q_1^{(2)}}\,\overline{n_1} - \overline{q_2^{(2)}}\,\overline{m_1} &= q_1^{(2)} a_0^{(2)},
\end{aligned} \tag{59}$$

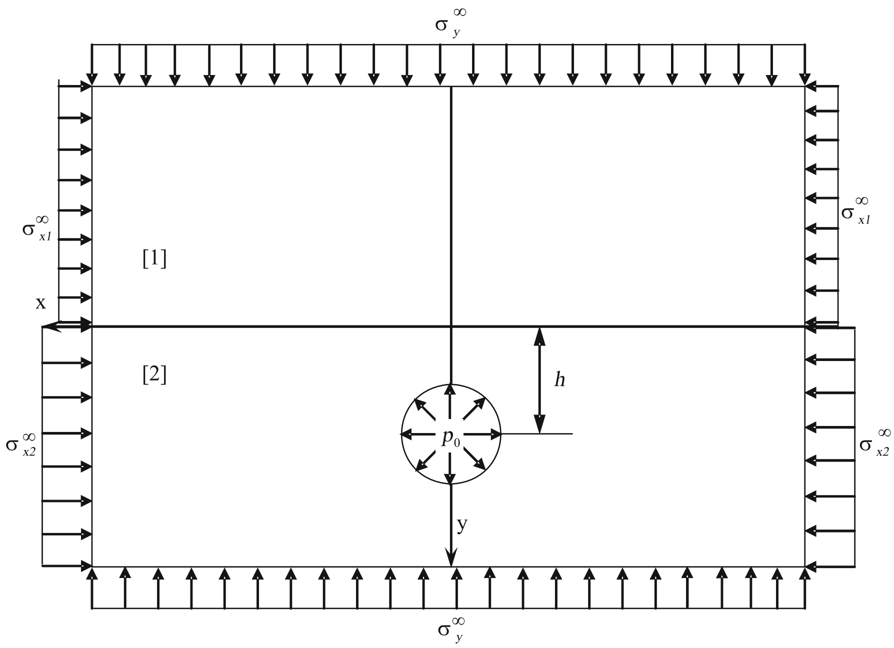

Fig. 3 Scheme of model problem with circular hole in an orthotropic sectionally homogeneous plane

$$
\begin{aligned}
s_2 + l_2 - \overline{n_2} - \overline{m_2} &= b_0^{(2)},\\
\mu_1^{(1)} s_2 + \mu_2^{(1)} l_2 - \overline{\mu_1^{(2)}}\,\overline{n_2} - \overline{\mu_2^{(2)}}\,\overline{m_2} &= \mu_2^{(2)} b_0^{(2)},\\
p_1^{(1)} s_2 + p_2^{(1)} l_2 - \overline{p_1^{(2)}}\,\overline{n_2} - \overline{p_2^{(2)}}\,\overline{m_2} &= p_2^{(2)} b_0^{(2)},\\
q_1^{(1)} s_2 + q_2^{(1)} l_2 - \overline{q_1^{(2)}}\,\overline{n_2} - \overline{q_2^{(2)}}\,\overline{m_2} &= q_2^{(2)} b_0^{(2)}.
\end{aligned} \tag{60}
$$

Let this system be solved. Then, the stress functions would be given by (58) and the stresses would be given by (52) and (53). These solutions were also obtained by other methods [4, 8, 10, 27].

3.2.2 Example

We consider sectionally homogeneous infinite media with a circular hole when the surface homogeneous pressure is applied as shown in the Fig. 3. It is assumed that the stresses at infinity take the following values:

$$\sigma_{xj}^{\infty}, \quad \sigma_y^{\infty} = \rho g H, \quad \tau_{xy}^{\infty} = 0.$$

The complex potentials have the following asymptotic far away from the contact surface:

$$\Phi_1^{(j)}(z_1) = \Gamma_1, \quad \Phi_2^{(j)}(z_2) = \Gamma_2,$$

where $\Gamma_i^{(j)}$ are constants to be defined.

The equations (60) yield the following system of equations:

$$\begin{aligned} 2Re[(\mu_1^{(j)})^2\Gamma_1 + (\mu_2^{(j)})^2\Gamma_2] &= \sigma_{xj}^{\infty}, \\ 2Re[\Gamma_1 + \Gamma_2] &= \sigma_y^{\infty}, \\ 2Re[\mu_1^{(j)}\Gamma_1 + \mu_2^{(j)}\Gamma_2] &= 0. \end{aligned} \tag{61}$$

The last equation of (61) holds if

$$2(\mu_1^{(j)}\Gamma_1 + \mu_2^{(j)}\Gamma_2) = ir_0^{(j)},$$

where $r_0^{(j)}$ is an arbitrary real constant. The system (61) can be easily solved and

$$\begin{aligned} \Gamma_1 &= i(r_0^{(1)}\mu_2^{(2)} - r_0^{(2)}\mu_2^{(1)})/\Delta, \\ \Gamma_2 &= i(r_0^{(2)}\mu_1^{(1)} - r_0^{(1)}\mu_1^{(2)})/\Delta, \end{aligned} \tag{62}$$

where $\Delta = \mu_1^{(1)}\mu_2^{(2)} - \mu_2^{(1)}\mu_1^{(2)}$. Substitution of (62) into the first equation of (61) yields

$$\begin{aligned} \delta_1 r_0^{(1)} + \delta_2 r_0^{(2)} &= -\frac{\sigma_{x_1}^{\infty}}{2}, \\ \delta_3 r_0^{(1)} + \delta_4 r_0^{(2)} &= -\frac{\sigma_{x_2}^{\infty}}{2}, \end{aligned} \tag{63}$$

where $\delta_1 = Im[((\mu_1^{(1)})^2\mu_2^{(2)} - (\mu_2^{(1)})^2\mu_1^{(2)})/\Delta]$, $\delta_2 = Im[(\mu_1^{(1)}\mu_2^{(1)}(\mu_2^{(1)} - \mu_1^{(1)})/\Delta]$, $\delta_3 = Im[(\mu_1^{(2)}\mu_2^{(2)}(\mu_1^{(2)} - \mu_2^{(2)})/\Delta]$, $\delta_4 = Im[((\mu_2^{(2)})^2\mu_1^{(1)} - (\mu_1^{(2)})^2\mu_2^{(1)})/\Delta]$.

Therefore,

$$r_0^{(1)} = \frac{\delta_1\sigma_{x_2}^{\infty} - \delta_4\sigma_{x_1}^{\infty}}{2(\delta_1\delta_4 - \delta_2\delta_3)}, r_0^{(2)} = \frac{\delta_3\sigma_{x_1}^{\infty} - \delta_1\sigma_{x_2}^{\infty}}{2(\delta_1\delta_4 - \delta_2\delta_3)}.$$

The second equation of (61) yields

$$(\delta_4\delta_5 - \delta_3\delta_6)\sigma_{x_1}^{\infty} + (\delta_1\delta_6 - \delta_2\delta_5)\sigma_{x_2}^{\infty} = (\delta_1\delta_4 - \delta_2\delta_3)\sigma_y^{\infty}, \tag{64}$$

where

$$\delta_5 = Im[(\mu_2^{(2)} - \mu_1^{(2)})/\Delta], \ \delta_6 = Im[(\mu_1^{(1)} - \mu_2^{(1)})/\Delta].$$

Let the condition $\sigma_{x1}^{\infty} = \sigma_{x2}^{\infty}$ hold at infinity. Then the value σ_x^{∞} is defined through σ_y^{∞}.

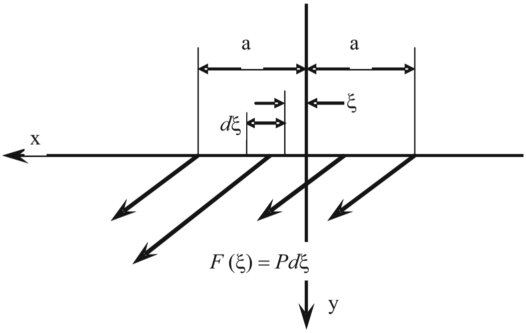

Fig. 4 Constant force acting on the segment

We will solve the source problem by the superposition principle for the following two stress states. The first one is the stress state in the media without a hole and the second one is characterized by the vanishing stresses at infinity and by the following boundary conditions on the hole surface:

$$\sigma_s = (-p_0 + \sigma_{x_2}^{\infty})\cos(n, y) - (\sigma_y^{\infty} - p_0)\cos(n, x),$$
$$\sigma_n = (-p_0 + \sigma_{x_2}^{\infty})\cos^2(n, x) + (\sigma_y^{\infty} - p_0)\cos^2(n, y). \tag{65}$$

Then, the full stresses are defined by formulae at the upper and lower half planes

$$\sigma_{x_2}^{(1)} = -\sigma_{x_1}^{\infty} + \sigma_x^{(1)}, \sigma_{y_2}^{(1)} = -\sigma_y^{\infty} + \sigma_y^{(1)}, \tau_{xy_2}^{(1)} = \tau_{xy}^{(1)},$$
$$\sigma_{x_2}^{(2)} = -\sigma_{x_2}^{\infty} + \sigma_x^{(2)}, \sigma_{y_2}^{(2)} = -\sigma_y^{\infty} + \sigma_y^{(2)}, \tau_{xy_2}^{(2)} = \tau_{xy}^{(2)}. \tag{66}$$

3.2.3 Method of Unknown Loads and its Numerical Realization

We consider a problem of the load uniformly distributed on the segment $|x| \leq a$ as shown in the Fig. 4. Let it be solved by the method presented in the previous section. Then, we define the stresses near the point (X_0, Y_0) as the functions of (x, y)

$$\sigma_x^{(j)} = X_0 A_x^{(j)}(x, y) + Y_0 B_x^{(j)}(x, y),$$
$$\sigma_y^{(j)} = X_0 A_y^{(j)}(x, y) + Y_0 B_y^{(j)}(x, y),$$
$$\tau_{xy}^{(j)} = X_0 A_{xy}^{(j)}(x, y) + Y_0 B_{xy}^{(j)}(x, y). \tag{67}$$

The following expressions for the stresses take place on the segment

$$\sigma_x^{(j)} = P_{X_0} I A_x^{(j)}(x, y) + P_{Y_0} I B_x^{(j)}(x, y),$$
$$\sigma_y^{(j)} = P_{X_0} I A_y^{(j)}(x, y) + P_{Y_0} I B_y^{(j)}(x, y),$$
$$\tau_{xy}^{(j)} = P_{X_0} I A_{xy}^{(j)}(x, y) + P_{Y_0} I B_{xy}^{(j)}(x, y), \tag{68}$$

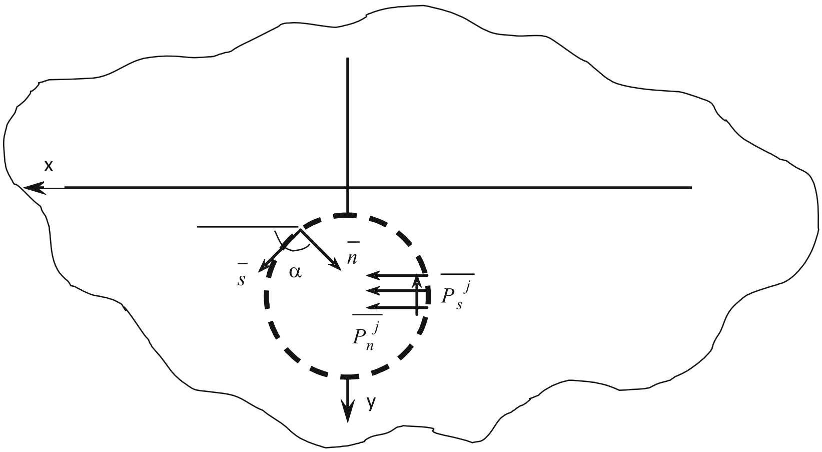

Fig. 5 Scheme of model problem solving

where

$$IA_x(j)(x,y)=\int_{-a}^{a}A_x^{(j)}(x-\xi,y)d\xi,\quad IA_y(j)(x,y)=\int_{-a}^{a}A_y^{(j)}(x-\xi,y)d\xi,$$

$$IB_x^{(j)}(x,y)=\int_{-a}^{a}B_x^{(j)}(x-\xi,y)d\xi,\quad IB_y^{(j)}(x,y)=\int_{-a}^{a}B_y^{(j)}(x-\xi,y)d\xi$$

$$IA_{xy}^{(j)}(x,y)=\int_{-a}^{a}A_{xy}^{(j)}(x-\xi,y)d\xi,\quad IB_{xy}^{(j)}(x,y)=\int_{-a}^{a}B_{xy}^{(j)}(x-\xi,y)d\xi,$$

$$P_{X_0}=\int_{-a}^{a}X_0d\xi,\quad P_{Y_0}=\int_{-a}^{a}Y_0d\xi.$$

The method of solution near the circular hole (see Fig. 5) can be presented as follows. First, the circle is divided onto N segments. Unknown constant shear and normal loads P_s^j and P_n^j are applied (to each small segment). Using (67) and (68) we can calculate the stresses at the middle points of each segment

$$\sigma_s^i=\Sigma_{k=1}^{N}A_{ss}^{ik}P_s^k+\Sigma_{k=1}^{N}A_{sn}^{ik}P_n^k,$$
$$\sigma_n^i=\Sigma_{k=1}^{N}A_{ns}^{ik}P_s^k+\Sigma_{k=1}^{N}A_{nn}^{ik}P_n^k,i=\overline{1,N}. \tag{69}$$

The values P_n^j and P_s^j can be found from the conditions at the centres of each element. As a result we obtain the following system of equations:

$$(-p_0+\sigma_{x_2}^{\infty})\cos(n,y)-(\sigma_y^{\infty}-p_0)\cos(n,x)=\Sigma_{k=1}^{N}A_{ss}^{ik}P_s^k+\Sigma_{k=1}^{N}A_{sn}^{ik}P_n^k,$$
$$(-p_0+\sigma_{x_2}^{\infty})\cos^2(n,x)+(\sigma_y^{\infty}-p_0)\cos^2(n,y)=\Sigma_{k=1}^{N}A_{ns}^{ik}P_s^k+\Sigma_{k=1}^{N}A_{nn}^{ik}P_n^k,$$
$$i=\overline{1,N}. \tag{70}$$

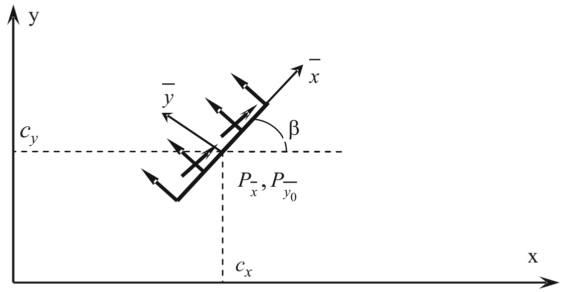

Fig. 6 Stresses caused by load of arbitrary orientation

Consider an example of the distributed force on the segment in the local coordinate system $(\overline{x}, \overline{y})$ shown in Fig. 6. The segment is defined by equations: $|\overline{x}| \leq a, y = 0$. The coordinate systems are related by equations

$$\overline{x} = (x - c_x)\cos(\beta) + (y - c_y)\sin(\beta), \overline{y} = -(x - c_x)\sin(\beta) + (y - c_y)\cos(\beta). \quad (71)$$

The stresses in the global coordinates have the form

$$\begin{aligned}\sigma_x &= \sigma_{\overline{x}}\cos^2(\beta) - 2\tau_{\overline{xy}}\sin(\beta)\cos(\beta) + \sigma_{\overline{y}}\sin^2(\beta),\\ \sigma_y &= \sigma_{\overline{x}}\sin^2(\beta) + 2\tau_{\overline{xy}}\sin(\beta)\cos(\beta) + \sigma_{\overline{y}}\cos^2(\beta),\\ \tau_{xy} &= (\sigma_{\overline{x}} - \sigma_{\overline{y}})\sin(\beta)\cos(\beta) + \tau_{\overline{xy}}\cos(2\beta). \end{aligned} \quad (72)$$

Moreover, we have

$$\begin{aligned}\sigma_x^{(j)} = P_{\overline{X_0}}(IA_x^{(j)}(\overline{x},\overline{y})\cos^2(\beta) - 2IA_{xy}^{(j)}(\overline{x},\overline{y})\cos(\beta)\sin(\beta) +\\ IA_y^{(j)}(\overline{x},\overline{y})\sin^2(\beta)) + P_{\overline{Y_0}}(IB_x^{(j)}(\overline{x},\overline{y})\cos^2(\beta) -\\ 2IB_{xy}^{(j)}(\overline{x},\overline{y})\cos(\beta)\sin(\beta) + IB_y^{(j)}(\overline{x},\overline{y})\sin^2(\beta)),\\ \sigma_y^{(j)} = P_{\overline{X_0}}(IA_x^{(j)}(\overline{x},\overline{y})\sin^2(\beta) + 2IA_{xy}^{(j)}(\overline{x},\overline{y})\cos(\beta)\sin(\beta) +\\ IA_y^{(j)}(\overline{x},\overline{y})\cos^2(\beta)) + P_{\overline{Y_0}}(IB_x^{(j)}(\overline{x},\overline{y})\sin^2(\beta) +\\ 2IB_{xy}^{(j)}(\overline{x},\overline{y})\cos(\beta)\sin(\beta) + IB_y^{(j)}(\overline{x},\overline{y})\cos^2(\beta)),\\ \tau_{xy}^{(j)} = P_{\overline{X_0}}((IA_x^{(j)}(\overline{x},\overline{y}) - IA_y^{(j)}(\overline{x},\overline{y}))\sin(\beta)\cos(\beta) +\\ IA_{xy}^{(j)}(\overline{x},\overline{y})(\cos^2(\beta) - \sin^2(\beta))) + P_{\overline{Y_0}}((IB_x^{(j)}(\overline{x},\overline{y}) -\\ IB_y^{(j)}(\overline{x},\overline{y}))\sin(\beta)\cos(\beta) + IB_{xy}^{(j)}(\overline{x},\overline{y})(\cos^2(\beta) - \sin^2(\beta))). \end{aligned} \quad (73)$$

In order to obtain the influence coefficients $IA_{xy}^{(j)}, IA_{xy}^{(j)}, \ldots$ we choose the point (x, y) as the centre of the jth element. The scheme for boundary elements is shown in Fig. 7. The local coordinates of the ith point relative to the jth point have the form

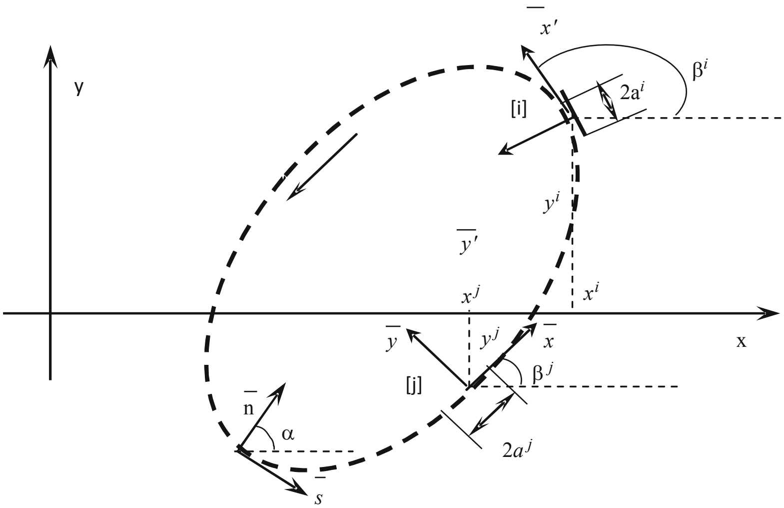

Fig. 7 Scheme for boundary elements

$$
\begin{aligned}
\overline{x} &= (x^i - x^j)\cos(\beta^j) + (y^i - y^j)\sin(\beta^j),\\
\overline{y} &= -(x^i - x^j)\sin(\beta^j) + (y^i - y^j)\cos(\beta^j)
\end{aligned}
\tag{74}
$$

The stress components at the ith point relative to the jth point can be obtained by (68)

$$
\begin{aligned}
\sigma_{\overline{x}}^{(k)i} &= P_{\overline{x}}^j IA_x^{(k)}(\overline{x},\overline{y}) + P_{\overline{y}}^j IB_x^{(k)}(\overline{x},\overline{y}),\\
\sigma_{\overline{y}}^{(k)i} &= P_{\overline{x}}^j IA_y^{(k)}(\overline{x},\overline{y}) + P_{\overline{y}}^j IB_y^{(k)}(\overline{x},\overline{y}),\\
\tau_{\overline{xy}}^{(k)i} &= P_{\overline{x}}^j IA_{xy}^{(k)}(\overline{x},\overline{y}) + P_{\overline{y}}^j IB_{xy}^{(k)}(\overline{x},\overline{y}),
\end{aligned}
\tag{75}
$$

where k is the number of the half-plane; i, j elements numbers. Ultimately, we have

$$
\begin{aligned}
\sigma_n^{i(k)} = {} & P_s^j(IA_x^{(k)}(\overline{x},\overline{y})\sin^2(\gamma) - IA_{xy}^{(k)}(\overline{x},\overline{y})\sin(2\gamma) + IA_y^{(k)}(\overline{x},\overline{y})\cos^2(\gamma)) + \\
& P_n^j(IB_x^{(k)}(\overline{x},\overline{y})\sin^2(\gamma) - IB_{xy}^{(k)}(\overline{x},\overline{y})\sin(2\gamma) + IB_y^{(k)}(\overline{x},\overline{y})\cos^2(\gamma)),\\
\sigma_s^{i(k)} = {} & P_s^j((IA_y^{(j)}(\overline{x},\overline{y}) - IA_x^{(j)}(\overline{x},\overline{y}))\frac{\sin(2\gamma)}{2} + IA_{xy}^{(j)}(\overline{x},\overline{y})\cos(2\gamma)) + \\
& P_n^j((IB_y^{(j)}(\overline{x},\overline{y}) - IB_x^{(j)}(\overline{x},\overline{y}))\frac{\sin(2\gamma)}{2} + IB_{xy}^{(j)}(\overline{x},\overline{y})\cos(2\gamma)),
\end{aligned}
\tag{76}
$$

where $\gamma = \beta_i - \beta_j$. So we can find the influence coefficients expressed through P_s^j and P_n^j in (76). Substituting them in (70) we arrive at a linear system. After its solution the stress–strain state can be explicitly determined.

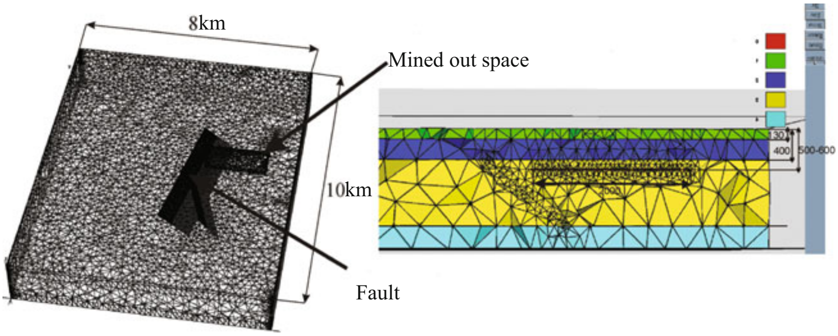

Fig. 8 Four layered massive

3.3 Three-dimensional Models of Conjugative Processes in Porous Media by Use of the Finite Element Method

We consider transversely an isotropic viscoelastic four-layered massif with intersection faults. There is also a mined out space. The scheme of the problem is displayed in Fig. 8. The second layer from the top has porous liquid in its skeleton. We investigate the flow in the massif skeleton when a mined external space is moved to the fault. The problem is described by the following equation:

1) Equilibrium equations with the fluid pressure have the form

$$\frac{\partial \sigma_{xx}}{\partial x} + \frac{\partial \sigma_{xy}}{\partial y} + \frac{\partial \sigma_{xz}}{\partial z} - \frac{\partial p}{\partial x} = 0,$$
$$\frac{\partial \sigma_{xy}}{\partial x} + \frac{\partial \sigma_{yy}}{\partial y} + \frac{\partial \sigma_{yz}}{\partial z} - \frac{\partial p}{\partial y} = 0,$$
$$\frac{\partial \sigma_{xz}}{\partial x} + \frac{\partial \sigma_{yz}}{\partial y} + \frac{\partial \sigma_{zz}}{\partial z} - \frac{\partial p}{\partial z} + \rho g = 0.$$

2) Storage equation with the pressure terms [25]

$$\frac{\partial p}{\partial t} = a\left(\frac{\partial^2 p}{\partial x^2} + \frac{\partial^2 p}{\partial y^2} + \frac{\partial^2 p}{\partial z^2}\right) - \alpha_p \frac{\partial}{\partial t}\left(\frac{\sigma_{xx} + \sigma_{yy} + \sigma_{zz}}{3}\right),$$

where $a = \frac{k(1+\varepsilon)}{\gamma(a_\nu + \varepsilon\beta)}$, $\alpha_p = \frac{a_\nu}{a_\nu + \varepsilon\beta}$, ε is the porosity coefficient, β is the fluid compressibility, a_ν is the rock hardening coefficient, k is the filtration coefficient, and t is time.

3) The physical law yields

$$\sigma_{xx} = \frac{1 - \nu_{pz}\nu_{zp}}{E_p E_z \Delta}\varepsilon_{xx} + \frac{\nu_p + \nu_{zp}\nu_{zp}}{E_p E_z \Delta}\varepsilon_{yy} + \frac{\nu_{zp} + \nu_{zp}\nu_{zp}}{E_p E_z \Delta}\varepsilon_{zz} + 2D(\dot{\varepsilon}_{xx} - \dot{\varepsilon}_0),$$
$$\sigma_{yy} = \frac{\nu_p + \nu_{zp}\nu_{zp}}{E_p E_z \Delta}\varepsilon_{xx} + \frac{1 - \nu_{pz}\nu_{zp}}{E_p E_z \Delta}\varepsilon_{yy} + \frac{\nu_{zp} + \nu_{zp}\nu_{zp}}{E_p E_z \Delta}\varepsilon_{zz} + 2D(\dot{\varepsilon}_{yy} - \dot{\varepsilon}_0),$$

$$\sigma_{zz} = \frac{\nu_{zp} + \nu_{zp}\nu_{zp}}{E_p E_z \Delta}\varepsilon_{xx} + \frac{\nu_{zp} + \nu_{zp}\nu_{zp}}{E_p E_z \Delta}\varepsilon_{yy} + \frac{1-\nu_p^2}{E_p^2 \Delta}\varepsilon_{zz} + 2D(\dot{\varepsilon}_{zz} - \dot{\varepsilon}_0),$$

$$\sigma_{xz} = 2G_{zp}\varepsilon_{xz} + 2D\dot{\varepsilon}_{xz}, \sigma_{yz} = 2G_{zp}\varepsilon_{yz} + 2D\dot{\varepsilon}_{yz}, \sigma_{xy} = \frac{E_p}{1+\nu_p}\varepsilon_{xy} + 2D\dot{\varepsilon}_{xy},$$

where E_p, and ν_p are Young's modulus and Poisson's ratio respectively in the horizontal plane; E_z, ν_{zp}, and G_{zp} are Young's modulus, Poisson's ratio, and the shear modulus in the vertical plane; $\nu_{pz} = \frac{E_p}{E_z}\nu_{zp}$;$\Delta = \frac{(1+\nu_p)(1-2\nu_{zp}\nu pz)}{E_p^2 Ez}$; and D is the viscosity coefficient. Here, the Kelvin model is used.

4) Compatibility equations

$$\frac{\partial^2\varepsilon_{xx}}{\partial y^2} + \frac{\partial^2\varepsilon_{yy}}{\partial x^2} = 2\frac{\partial^2\varepsilon_{xy}}{\partial x\partial y},$$

$$\frac{\partial^2\varepsilon_{xx}}{\partial z^2} + \frac{\partial^2\varepsilon_{zz}}{\partial x^2} = 2\frac{\partial^2\varepsilon_{xz}}{\partial x\partial z},$$

$$\frac{\partial^2\varepsilon_{zz}}{\partial y^2} + \frac{\partial^2\varepsilon_{yy}}{\partial z^2} = 2\frac{\partial^2\varepsilon_{yz}}{\partial z\partial y},$$

$$\frac{\partial^2\varepsilon_{xx}}{\partial y\partial z} - \frac{\partial^2\varepsilon_{xy}}{\partial x\partial z} - \frac{\partial^2\varepsilon_{xz}}{\partial x\partial y} + \frac{\partial^2\varepsilon_{yz}}{\partial x^2} = 0,$$

$$\frac{\partial^2\varepsilon_{zz}}{\partial x\partial y} - \frac{\partial^2\varepsilon_{xz}}{\partial y\partial z} - \frac{\partial^2\varepsilon_{yz}}{\partial x\partial z} + \frac{\partial^2\varepsilon_{xy}}{\partial z^2} = 0,$$

$$\frac{\partial^2\varepsilon_{yy}}{\partial x\partial z} - \frac{\partial^2\varepsilon_{xy}}{\partial y\partial z} - \frac{\partial^2\varepsilon_{yz}}{\partial x\partial y} + \frac{\partial^2\varepsilon_{xz}}{\partial y^2} = 0.$$

5) Cauchy's relations

$$\varepsilon_{ij} = \frac{1}{2}\left(\frac{\partial u_i}{\partial x_j} + \frac{\partial u_j}{\partial x_i}\right).$$

6) Boundary and initial conditions:
   a) On the left and right edges, i.e. with $y = Y_s$, $y = Y_n$: $\sigma_{yz} = \sigma_{xy} = 0$, $u_y = 0$, $p = 0$
   b) On the front and back edges, i.e. with $x = X_w$, $x = X_e$: $\sigma_{xz} = \sigma_{yx} = 0$,$u_x = 0$,$p = 0$
   c) At the bottom: $u_x = u_y = u_z = 0$
   d) At the upper surface: $\sigma_{xz} = \sigma_{yz} = \sigma_{zz}$
   e) At the boundary of the water layer with the massif–impermeability condition $\frac{\partial p}{\partial n} = 0$
   f) $p = 0$ for $t = 0$
   g) Contact conditions on the faults surfaces

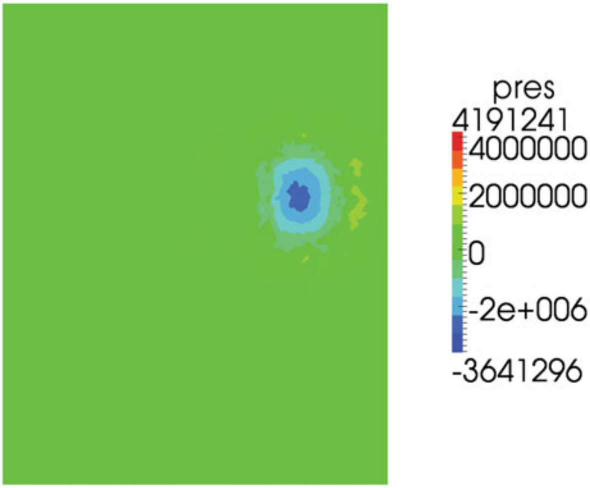

Fig. 9 Pressure distribution in horizontal plane after third step of deleting elements

$$\sigma_{n1} = \sigma_{n2},$$
$$u_{n1} = u_{n2},$$
$$\sigma_{\tau 1} = \sigma_{\tau 2},\ |\sigma_\tau| < f\sigma_n,$$
$$u_{\tau 1} = u_{\tau 2},\ |\sigma_\tau| < f\sigma_n,$$
$$\sigma_{\tau 1} = \sigma_{\tau 2} = f\sigma_n,\ |\sigma_\tau| > f\sigma_n.$$

Here, σ_n and σ_τ are the normal and shear stresses and f is the friction coefficient. We are interested only in the additional pressure, which is caused by mining works. Hence, we impose vanishing boundary and initial conditions for the pressure.

The problem is solved by a finite element package using the following scheme:

1) Calculate the initial stress–strain state of the massif caused by gravity. Hydromechanical processes are not considered at this stage.
2) Step-by-step deletion of the elements which model the mined out space. Dimensions of the mined out space are $2000 \times 2000 \times 10\ \mathrm{m}^3$. And on each step we delete elements of size $l \times 2000 \times 10\ \mathrm{m}^3$. Hence, the mined out space is in movement to the fault (on the first step $l = 1200$ m and on the following steps $l = 200$ m). The velocity of movement is 1 km/year.
3) Calculation of the moment when the steady state of the massif is reached. We used the following as the physical, mechanical, and geometry parameters of the layers:
   First layer: $E_p = 0.3(GPa)$, $E_z = 1(GPa)$, $\nu_p = \nu_{zp} = 0.3$, $G_{zp} = 0.0577(GPa)$, $top = 0$, $bottom = -130$ m,
   Second layer: $E_p = 5(GPa)$, $E_z = 5(GPa)$, $\nu_p = \nu_{zp} = 0.3$, $G_{zp} = 0.288(GPa)$, $top = -130$, $bottom = -400$ m,
   Third layer: $E_p = 14(GPa)$, $E_z = 14(GPa)$, $\nu_p = \nu_{zp} = 0.3$, $G_{zp} = 0.8(GPa)$, $top = -400$, $bottom = -1800$ m,

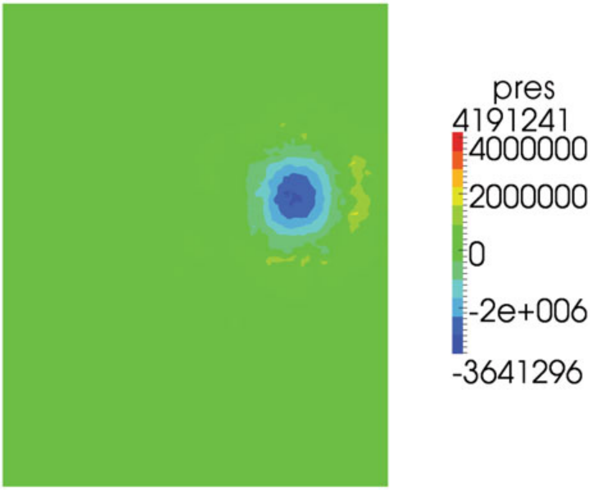

Fig. 10 Pressure distribution in horizontal plane after fifth step of deleting elements

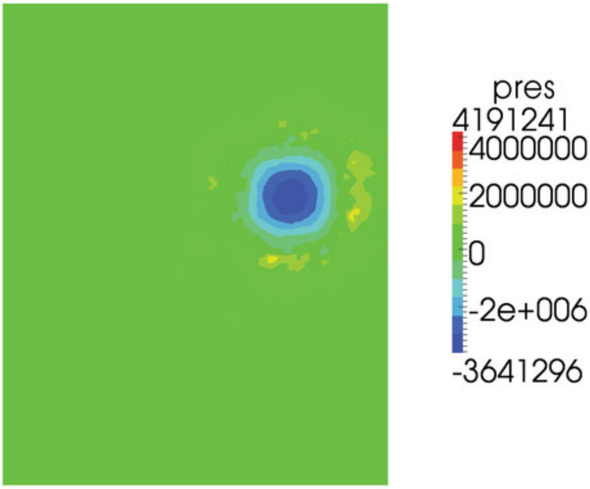

Fig. 11 Pressure distribution in horizontal plane after last step of deleting elements

Fourth layer: $E_p = 14(GPa)$, $E_z = 14(GPa)$, $\nu_p = \nu_{zp} = 0.3$, $G_{zp} = 0.8(GPa)$, $top = -1800$, $bottom = -2200$ m.

The fluid properties of the second layer are expressed by the parameters

$$k = 10^{-9}\,(m/s),\ \beta = 10^{-10}\,(Pa^{-1}),\ \varepsilon = 0.11,\ a_\nu = 10^{-9}\,(Pa^{-1})$$

Distribution of fluid pressure is shown In Figs. 9, 10, 11, 12, 13 and 14 at the horizontal plane on the depth 250 m and at the vertical plane the middle of the mined out space perpendicular to the x direction.

Remark: The fluid pressure has the same sign as the stresses, hence, at the compressible pressure is negative.

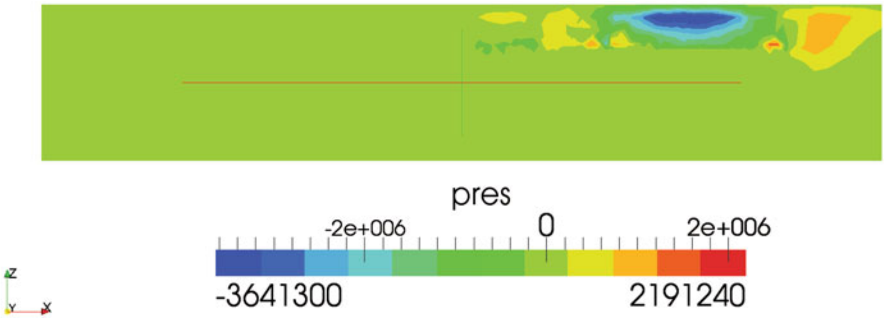

Fig. 12 Pressure distribution in vertical plane in the third step of deleting elements

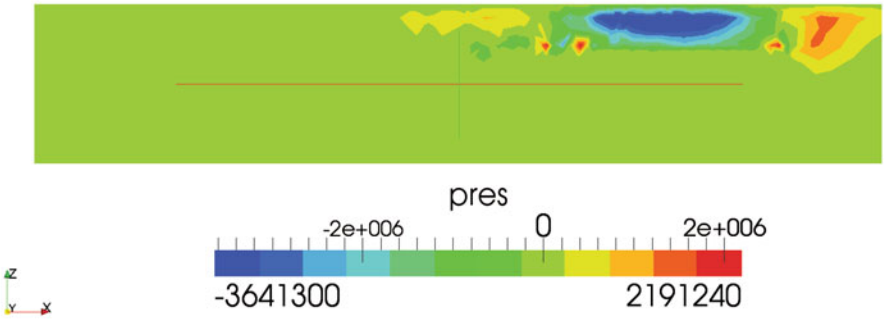

Fig. 13 Pressure distribution in horizontal plane after fifth step of deleting elements

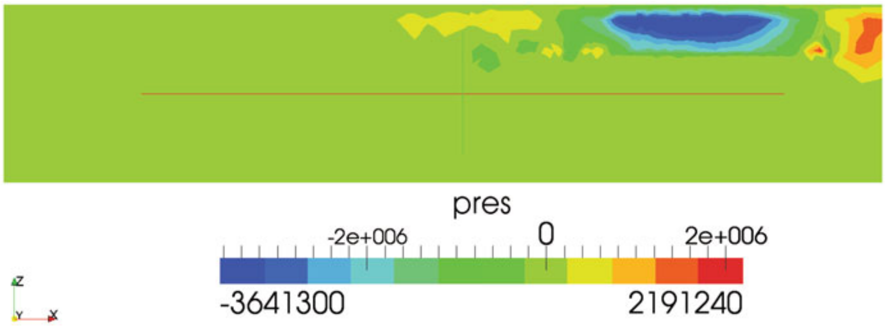

Fig. 14 Pressure distribution in horizontal plane after last step of deleting elements

One can see from the graphics that the water layer is in zones with high horizontal stresses, because large sizes of the mined out space of compressible horizontal stresses are greater than the tension of vertical stresses. Therefore, the additional pressure of fluid is positive in the usual sense. We can also see the influence of the fault on the pressure distribution because the pressure distribution is different on both sides of the fault.

The problem is solved by use of the finite difference approximation in time; a finite element method is used at each time step for spacial variables. The package $Tochnog^{©}$ is used for implementation of the finite element method.

Acknowledgements The authors are grateful to Dr. V.A. Savenkov for fruitful discussions during the preparation of the chapter.

References

1. Adler, P.M.: Porous Media. Geometry and Transport. Butterworth-Heinemann, Stoneham (1992)
2. Adler, P.M., Thovert, J.-F., Mourzenko, V.V.: Fractured Porous Media. Oxford University Press, Oxford (2012)
3. Bardzokas, D.I., Filshtinsky, M.L., Filshtinsky, L.A.: Mathematical Methods in Electro-Magneto-Elasticity. Springer, Berlin (2007)
4. Becker, W.: Green's functions for the anisotropic half-plane loaded by a single force. J. Ing. Arch. **60**, 255–261 (1990)
5. Berlyand, L., Kolpakov, A.G., Novikov, A.: Introduction to the Network Approximation Method for Materials Modeling. Cambridge University Press, Cambridge (2012)
6. Bojarski, B.: On generalized Hilbert boundary value problem. Soobsch. AN GruzSSR **25**, 385–390 (1960) (In Russian)
7. Cherdancev, N.V.: Damage zones in the region of conjugation of two mined out spaces. J. Appl. Mech. Tech. Phys. **45**, 137–139 (2004)
8. Chow, Y.T., Pande, C.S.: Interfacial screw dislocation in anisotropic two-phase media. J. Appl. Phys. **44**, 3355–3356 (1973)
9. Erzhanov, G.S., Saginov, A.S., Veksler, Y.A.: About mechanism of suddenly ejection of gas and coal. J. Min. Sci. **4**, 3–6 (1973)
10. Frasier, J.T.: Force in the plane of two joined semi-infinite plates. J. Appl. Mech. **24**, 582–584 (1957)
11. Gakhov, F.D.: Boundary Value Problems. Pergamon (Addison-Wesley), Oxford (1966)
12. Grigolyuk, E.I., Filshtinsky, L.A.: Periodical Piece–Homogeneous Elastic Structures. Nauka, Moscow (1991) (In Russian)
13. Grigolyuk, E.I., Filshtinsky, L.A.: Regular Piece-Homogeneous Structures with Defects. Fiziko-Matematicheskaja Literatura, Moscow (1994) (In Russian)
14. Kalamkarov, A.L., Andrianov, I.V., Danishevskyy, V.V.: Asymptotic Homogenization of Composite Materials and Structures. Appl. Mech. Rev. **62**, 030802 (2009) (20 p.)
15. Kolpakov, A.A., Kolpakov, A.G.: Capacity and Transport in Contrast Composite Structures. CRC, Boca Raton (2009)
16. Kosmodamianskii, A.S., Kaloerov, S.A.: Thermal Stresses in Multiply Connected Plates. Rik, Kiev (1983) (In Russian)
17. Lechnicki, S.: Theory of Elasticity of Anisotropic Bodies. Nauka, Moscow (1977)
18. Lindin, G.L., Kvochin, V.A.: Stress distribution near mining. Int. J. Tech. Technol. Min. **7**, 40–48 (2005)
19. Mikhlin, S.G.: Integral Equations. Pergamon, New York (1964)
20. Mityushev, V.: Conductivity of a two-dimensional composite containing elliptical inclusion. Proc. R. Soc. A **465**, 2991–3010 (2009)
21. Mityushev, V.: $\mathbb{R}$–linear and Riemann–Hilbert problems for multiply connected domains. In: Rogosin, S.V., Koroleva, A.A. (eds.) Advances in Applied Analysis, pp. 147–176. Birkhäuser, Basel (2012)

22. Mityushev, V.V., Rogosin, S.V.: Constructive Methods for Linear and Nonlinear Boundary Value Problems for Analytic Functions Theory. Chapman & Hall/CRC, Boca Raton (2000)
23. Muskhelishvili, N.I.: Some Problems of Mathematical Theory of Elasticity Effective Substances. Nauka, Moscow (1999)
24. Prusov, I.: Thermoelastic Anisotropic Plates. BSU, Minsk (1978)
25. Shestakov, V.: Dynamic of Undeground Waters. MSU, Moscow (1979)
26. Smith, B., Björstad, P., Gropp, W.: Domain Decomposition: Parallel Multilevel Methods for Elliptic Partial Differential Equations. Cambridge University Press, Cambridge (1996)
27. Tewary, V.K., Wagoner, R.H., Hirth, J.P.: Elastic Green's function for a composite solid with a planar interface. J. Math. Res. **4**, 113–123 (1989)
28. Ucin, G.E.: Analysis of stress state near mining in rock massif. J. Phys. Mesomech. **8**, 83–88 (2005)
29. Zelensky, V.S.: 3-D stability of rock massif in neighbourhood of horizontal parallel minings. J. News Nat. Acad. Sci. Ukr. **6**, 38–41 (2006)
30. Zhuravkov, M.: Mathematical Modeling of Deformation Processes in Rigid Deformable Bodies. BSU, Minsk (2002)

Springer
http://www.springer.com/978-1-4939-1245-2

Handbook of Functional Equations
Functional Inequalities
Rassias, T.M. (Ed.)
2014, XI, 555 p. 19 illus., 7 illus. in color., Hardcover
ISBN: 978-1-4939-1245-2